





CLINICAL INVESTIGATIVE STUDY

Cerebral blood flow in patients recovered from mild COVID-19

Souvik Sen  | Roger Newman-Norlund | Nicholas Riccardi | Christopher Rorden | Sarah Newman-Norlund  | Sara Sayers | Julius Fridriksson | Makenzie Logue

Department of Neurology, University of South Carolina, Columbia, South Carolina, USA

Correspondence

Souvik Sen, Department of Neurology, University of South Carolina School of Medicine, 8 Medical Park, Suite 420, Columbia, SC 29203, USA.

Email: Souvik.Sen@uscmed.sc.edu

This original finding has not been published elsewhere prior to this submission.

Funding information

University of South Carolina

Abstract

Background and Purpose: Cerebral hypoperfusion has been described in both severe and mild forms of symptomatic Coronavirus Disease 2019 (COVID-19) infection. The purpose of this study was to investigate global and regional cerebral blood flow (CBF) in asymptomatic COVID-19 patients.

Methods: Cases with mild COVID-19 infection and age-, sex-, and race-matched healthy controls were drawn from the Aging Brain Consortium at The University of South Carolina data repository. Demographics, risk factors, and data from the Montreal Cognitive Assessment were collected. Mean CBF values for gray matter (GM), white matter (WM), and the whole brain were calculated by averaging CBF values of standard space-normalized CBF image values falling within GM and WM masks. Whole brain region of interest-based analyses were used to create standardized CBF maps and explore differences between groups.

Results: Twenty-eight cases with prior mild COVID-19 infection were compared with 28 controls. Whole-brain CBF (46.7 ± 5.6 vs. 49.3 ± 3.7 , $p = .05$) and WM CBF (29.3 ± 2.6 vs. 31.0 ± 1.6 , $p = .03$) were noted to be significantly lower in COVID-19 cases as compared to controls. Predictive models based on these data predicted COVID-19 group membership with a high degree of accuracy (85.2%, $p < .001$), suggesting CBF patterns are an imaging marker of mild COVID-19 infection.

Conclusion: In this study, lower WM CBF, as well as widespread regional CBF changes identified using quantitative MRI, was found in mild COVID-19 patients. Further studies are needed to determine the reliability of this newly identified COVID-19 brain imaging marker and determine what drives these CBF changes.

KEYWORDS

cerebral blood flow, COVID-19, infection, white matter

INTRODUCTION

Central nervous system (CNS) involvement in severe acute respiratory syndrome coronavirus 2 (SARS-CoV-2) infection, as noted in the Coronavirus Disease 2019 (COVID-19) pandemic, has been increasingly recognized in the literature for possible mechanisms of neuroinvasion, neurotropism, and neurovirulence.¹ Critically ill COVID-19 patients, who experience severe hypoxia state and an inflammatory/cytokine

storm, often have more severe CNS injury and systemic complications. In comparison, patients with milder infection and no specific neurological symptoms in the acute phase typically have better clinical outcomes.² The advent of vaccination and less virulent strains of COVID-19 (eg, Omicron) has led to milder COVID-19 infection.^{3,4} Although patients with mild COVID-19 without any neurological manifestations appear to make complete recovery, limited data are available on their global and regional cerebral blood flow (CBF).

This is an open access article under the terms of the [Creative Commons Attribution-NonCommercial](https://creativecommons.org/licenses/by-nc/4.0/) License, which permits use, distribution and reproduction in any medium, provided the original work is properly cited and is not used for commercial purposes.

© 2023 The Authors. *Journal of Neuroimaging* published by Wiley Periodicals LLC on behalf of American Society of Neuroimaging.



Based on the literature, cerebral perfusion abnormalities in CNS viral infections vary from high to low CBF, depending on the implicated virus. An increase in CBF has been demonstrated in most cases, namely, herpes simplex virus and tick-borne encephalitis, while a reduction in CBF occurs with human immunodeficiency virus infection.⁵ With COVID-19 infection, at least three patterns of cerebral perfusion abnormalities have been reported: (1) in the early encephalitis phase, *N*-isopropyl-[123I]p-iodoamphetamine (123I-IMP) SPECT studies show cerebral hyperperfusion is possibly related to inflammation⁶; (2) in the later recovery phase, those with severe initial COVID-19 infection show global hypoperfusion that correlates with poor recovery outcome⁷; and (3) those with milder initial COVID-19 infection show white matter (WM) tract changes, possibly resulting from WM ischemia-hypoxia or immune-mediated inflammatory demyelination.⁸ The purpose of the current study was to investigate global and regional WM and gray matter (GM) hypoperfusion in a group of patients with milder COVID-19 infection.

METHODS

Participants

Data from 56 participants, half of whom were diagnosed with COVID-19 ($N = 28$) and half of whom were healthy control participants ($N = 28$), were drawn from the Aging Brain Cohort at The University of South Carolina (ABC@UofSC) data repository.⁹ Given evidence from prior studies that CBF measures can significantly vary as a function of age and sex, we ensured that the two samples were matched in terms of these demographic variables. All participants were native English speakers, were predominantly right-handed, and reported no abnormal neurological conditions or history of brain injury. COVID-19 severity, which was treated as an ordinal variable in our models, was based on self-report and fell into one of five categories: (1) participant received no treatment of any kind ($N = 4$); (2) participant used over the counter medicines for symptoms ($N = 15$); (3) participant visited a doctor and used prescribed medicines ($N = 3$); (4) participant visited urgent care or the emergency room (not admitted) ($N = 6$); and (5) participants admitted to a hospital ($N = 0$).

Standard protocol approvals and patient consents

All study participants consented to participate in the ABC@UofSC data repository. The institutional review board at the University of South Carolina approved both the original ABC@UofSC study as well as the use of the current data set from the repository.

MRI data collection

All neuroimaging data (T1-structural scan and arterial spin labeling [ASL] scan) were obtained from the data repository associated with the ABC@UofSC study, an ongoing cross-sectional cohort study at

the University of South Carolina. MRI data were collected at the McCausland Center for Brain Imaging located at Prisma Health Richland Hospital, Columbia, SC, using a Siemens 3T Prisma Fit scanner equipped with a 20-channel head coil. Foam cushions were used to stabilize participants' heads and minimize unwanted movement during scanning. The multi-echo, T1-weighted structural image had the following parameters: repetition time (TR) = 25.30 ms, inversion time (TI) = 1100 ms, echo time (TE) = (1.44, 2.9, 4.36, 5.82, and 7.28 ms), flip angle = 7.0 degrees, $256 \times 192 \times 256$ mm resolution, 1-mm isotropic voxel size, Generalized Autocalibrating Partial Parallel Acquisition (GRAPPA) $\times 2$, interleaved ascending acquisition with anterior-posterior (A \gg P) phase encoding, duration 6 minutes and 7 seconds. The Arterial Spin-labeled sequence was collected with the following settings: 97 volumes, TR = 5000 ms, TE = 14 ms, flip angle = 90 degrees, slices = 24, distance factor = 10%, $220 \times 220 \times 119$ mm resolution, $3.4 \times 3.4 \times 4.5$ mm voxel size, 6/8 phase partial Fourier, interleaved ascending acquisition with A \gg P phase encoding, bolus duration = 700 ms, inversion time = 1800 ms, 6-postlabeling delay (PLD) (400, 725, 1050, 1350, 1675, and 2000 ms), duration = 8 minutes and 7 seconds. Results from a 42-second time-of-flight scan (40 slices, TR = 21 ms, TE = 3.43 ms, flip angle = 30 degrees, -50% distance factor, $263 \times 350 \times 350$ mm resolution, $0.3 \times 0.3 \times 1.3$ mm voxel size, to positioning of the tagging plane for the ASL sequence, GRAPPA $\times 3$) were manually inspected and used to guide placement of the ASL tagging plane. Specifically, the tagging plane was always placed in a location at which the internal and external carotid arteries were not twisting, that is, travelling orthogonal to the Head-Foot axis. There were no strokes/neurological abnormalities/incidental findings in any of the participants.

MRI data analysis

MRI data were processed using the publicly available *nii_preprocess* pipeline, which has been used in numerous prior publications.¹⁰ For the current study, we were interested in examining differences in CBF between participants diagnosed with COVID-19 and a healthy, age- and sex-matched control sample. Using the ASL sequences described above, CBF data (perfusion-weighted images and calibrated perfusion-weighted images) were computed using FSL's Bayesian Inference for Arterial Spin Labeling (BASIL) tool.^{11,12} This tool was developed to specifically support processing of the 6-PSL pseudocontinuous ASL sequences developed by Oxford and used in the current study. We used BASIL's recommended (default) preprocessing settings as described in the ASL "white paper."¹³ BASIL output (ie, calibrated CBF volume maps in a standard space) was saved. Mean CBF values for GM, WM, and the whole brain were calculated by averaging CBF values of standard space-normalized CBF image values falling within GM and WM masks (90% tissue match probability), constructed using FSL's FAST segmentation algorithm applied to the Montreal Neurological Institute brain template.¹⁴ GM and WM regions of interest (ROIs) were derived from the Johns Hopkins University's (JHU) whole brain atlas. The JHU atlas has 189 total brain regions (<https://github.com/neuroimaging/niiStat/blob/master/roi/jhu.txt>).



Statistical analysis

Demographics including age, sex, and race as well as the investigated additional covariates including hypertension, diabetes, smoking status, current alcohol use, and Montreal Cognitive Assessment (MOCA) were assessed. The COVID-19 and control groups were compared using independent-sample *t*-test for continuous variables and Fisher's exact test for categorical variables. All data analysis for this study was completed using SAS version 9.4 (SAS institute Inc., Cary, NC).

Data files created using `nii_preprocess`¹⁰ were interrogated using our freely available machine-learning-based analysis tool, NiiStat.¹⁵ Briefly, we used support vector machine (SVM) learning to identify differences between COVID-19 and control groups and evaluate our ability to predict group membership using a leave-one-out approach (ie, our model was trained on the data of all individuals but one, and then attempted to identify group membership of the left-out individual).¹⁶ We also used support vector regression (SVR)¹⁷ to evaluate the relationship between regional GM and WM CBF with COVID-19 severity levels in the COVID-19 group.

Data availability and access statement

The Principal Author has full access to the data used in the analyses in the manuscript. The authors take full responsibility for the data, the analyses and interpretation, and the conduct of the research; they have full access to all of the data; and they have the right to publish any and all data, separate and apart from the guidance of any sponsor. Anonymized data not published within this article will be made available by request from any qualified investigator. Related documents such as study protocol and statistical analysis plan will be shared on reasonable request within 2 years of publication. The data will be made available for a similar period, and criteria for accessing data requires a written request to the ABC@USC investigator from all potential investigators.

RESULTS

A total of 56 participants were selected from the cohort of the ABC@USC study who consented and completed the MRI CBF measurement and MOCA testing, including 28 cases with mild COVID-19 infection (mean age \pm standard deviation [SD] = 44.3 \pm 19.5, 89% women) and 28 age- and sex-matched controls (mean age \pm SD = 44.9 \pm 19.8, 89% women), enrolled prior to the COVID-19 pandemic. Data from healthy adults were collected between August 2019 and March 2020, while data from participants with COVID-19 were collected between October 2020 and March 2021. Key demographic and health variables for the two groups are shown in Table 1 and self-reported vascular risk factors for cases and controls at baseline are shown in Table 1. The proportion of subjects with hypertension, diabetes, smoking, and alcohol use was similar across cases and controls. The MOCA score was similar ($p = .52$) between cases

TABLE 1 Baseline characteristics.

	COVID-19 mild infection (N = 28)	Control (N = 28)	<i>p</i> -value
Age	44.3 \pm 19.5 (20, 70)	44.9 \pm 19.8 (21, 69)	.90
Sex	Women = 25 (89%)	Women = 25 (89%)	1.0
	Men = 3 (11%)	Men = 3 (11%)	1.0
Race	White = 24	White = 24	.56
	Black = 4	Black = 3	.56
	Hispanic = 5	Hispanic = 1	.56
Hypertension	4 (14%)	5 (18%)	.72
Diabetes	1 (3%)	1 (3%)	1.0
Smoking	1 (3.6%)	2 (7.2%)	.55
Alcohol abuse	0 (0%)	0 (0%)	1.0
MOCA score values	27.71 \pm 1.8 (24, 30)	27.32 \pm 2.6 (19, 30)	.52

Note: Values are expressed as mean \pm standard deviation, or number of subjects. Percentage or range is shown in parentheses.

Abbreviations: COVID-19, Coronavirus Disease 2019; MOCA, Montreal Cognitive Assessment; N, number of subjects.

TABLE 2 Cerebral blood flow results.

	COVID-19 mild infection (N = 28)	Control (N = 28)	<i>p</i> -value
CBF (mL/100 g/min)			
White matter	29.3 \pm 2.6	31.0 \pm 1.6	.03
Gray matter	64.2 \pm 8.9	67.6 \pm 6.0	.10
Whole brain	46.7 \pm 5.6	49.3 \pm 3.7	.05

Note: All data are presented as mean \pm standard deviation, and *p*-values are reported for independent-sample *t*-tests (two-tailed). Listed *p*-values are based on a series of three, planned, independent-sample *t*-tests (two-tailed). Abbreviations: CBF, cerebral blood flow; COVID-19, Coronavirus Disease 2019; N, number of subjects.

(mean \pm SD = 27.7 \pm 1.8) and the controls (mean \pm SD = 27.3 \pm 2.6). CBF in the whole brain (46.7 \pm 5.6 vs. 49.3 \pm 3.7, $p = .05$) and WM (29.3 \pm 2.6 vs. 31.0 \pm 1.6, $p = .03$) was noted to be significantly lower in the COVID-19 cases compared with control group (Table 2). Blood flow in the GM was not significantly different between the two groups, although there was a slight trend toward lower CBV in the COVID-19 group, GM (64.2 \pm 8.9 vs. 67.6 \pm 6.0, $p = .10$). The differences in the mean were statistically significant in WM ($p = .03$) and were of borderline significance ($p = .05$) in the whole brain. Representative calibrated CBF maps from three participants each in COVID-19 and control group are shown in Figure 1.

Univariate analyses of the CBF differences between COVID-19 and controls using all GM and WM ROIs from the JHU whole brain atlas with $p < .05$ are depicted in Table 3. ROIs in the GM/WM and left/right side of the brain are depicted. Areas where the COVID-19 sample had significantly lower CBF than the control group in the univariate analysis are depicted by z-score color-coded map in Figure 2. A list

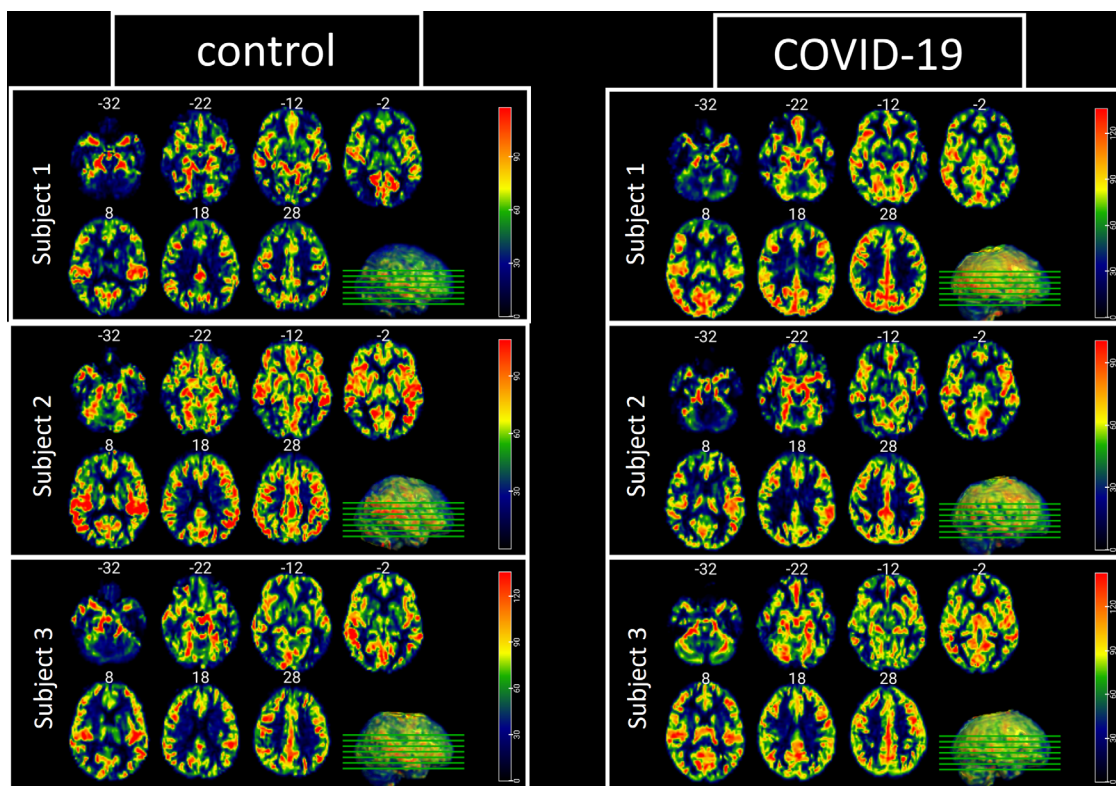


FIGURE 1 Representative calibrated CBF maps from three participants in each group. These data were generated using the Bayesian Inference for Arterial Spin Labelling processing pipeline. Color bar values represent mL/100 g/minute of cerebral blood flow.

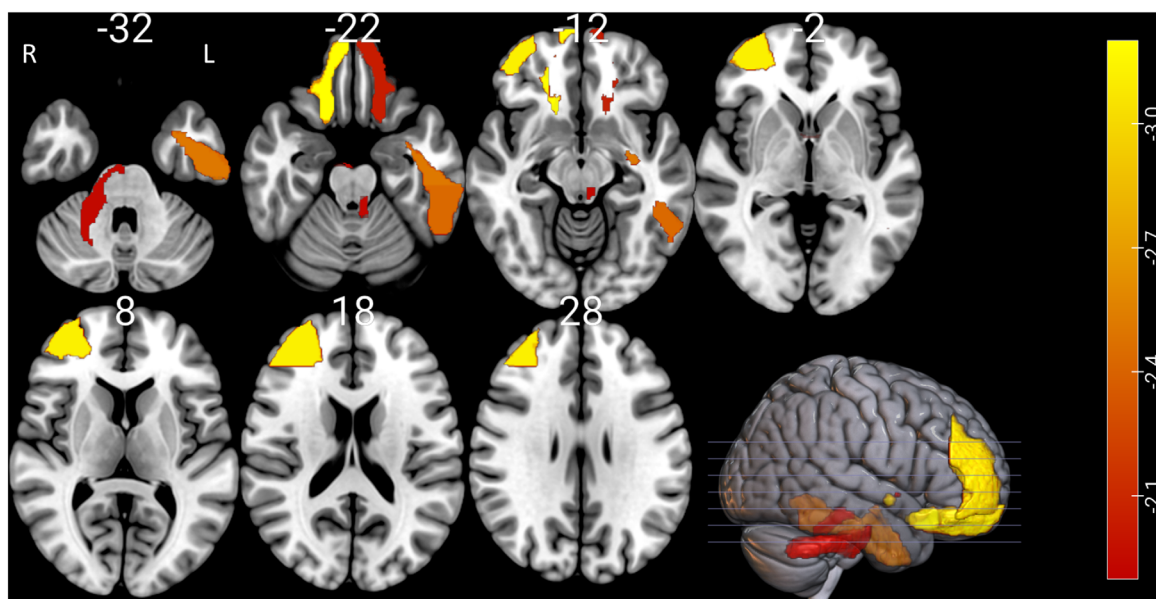


FIGURE 2 Areas where the COVID-19 group had significantly lower cerebral blood flow than the control group. White numbers indicate axial slice location. The color bar represents the z-scores for this contrast. Only statistically significant regions are shown. Data are derived from univariate analysis. R, right; L, left.



TABLE 3 Univariate results showing CBF differences between the control and COVID-19 groups.

Gray matter		
Left hemisphere	Posterior inferior temporal gyrus	-4.57
	Inferior temporal gyrus	-4.51
	Middle temporal gyrus	-3.81
	Entorhinal cortex	-3.15
	Globus pallidus	-3.1
Right hemisphere	Subgenual anterior cingulate	-3.06
	Subcallosal anterior cingulate	-3.58
	Middle fronto-orbital gyrus	-3.4
	Middle frontal gyrus	-3.24
	Middle frontal gyrus	-3.18
White matter		
Left hemisphere	Lenticular fasciculus	-4.17
	Genu of corpus callosum	-4.07
	Posterior thalamic radiation	-3.62
	Optic tract	-3.42
	Middle cerebellar peduncle	-3.36
	Inferior cerebellar peduncle	-3.26
	Superior cerebellar peduncle	-3.25
	Fornix	-3.19
	Sagittal stratum	-3.19
	Superior longitudinal fasciculus	-3.15
	Anterior commissure	-3.15
	Cingulum	-3.09
	Retrolenticular internal capsule	-3.07
Right hemisphere	Lenticular fasciculus	-3.85
	Genu of corpus callosum	-3.79
	Olfactory radiation	-3.57
	Optic tract	-3.37
	Fornix	-3.27
	Anterior corona radiata	-3.07
	Retrolenticular internal capsule	-3.07
	Middle cerebellar peduncle	-3.01
	Sagittal stratum	-2.99

Note: These values of gray matter and white matter regions are from the Johns Hopkins's University atlas. All listed results are $p < .05$, permutation corrected (1000 permutations). All regions indicated lower CBF in the COVID-19 group.

of regions most informative for the SVM model when classifying participants into control or COVID-19 groups is depicted in Table 4. Controls were identified with 77.4% accuracy, while COVID-19 participants were identified with 85.2% accuracy (overall classification $p < .0001$). Top 10 areas predictive of control group membership in the SVM model are also depicted in a color-coded map (Figure 3A), whereas the 10 areas predictive of COVID-19 group membership in

TABLE 4 List of regions most informative for the support vector machine model when classifying participants into control or COVID-19 groups.

Top 10 regions informative of control group membership	
Region	Feature weight
Right Meynert nucleus	3.21
Right pontine crossing tract	2.99
Right angular gyrus	2.38
Right uncinate fasciculus	2.30
Left amygdala	2.24
Right superior parietal gyrus	1.98
Left inferior frontal gyrus (pars opercularis)	1.93
Right precuneus	1.76
Left supramarginal gyrus	1.76
Left pontine crossing tract	1.74
Top 10 regions informative of COVID-19 group membership	
Region	Feature weight
Right middle fronto-orbital gyrus	-3.28
Right middle frontal gyrus	-3.12
Left lenticular fasciculus	-3.06
Left inferior temporal gyrus	-2.43
Left middle fronto-orbital gyrus	-2.05
Left anterior commissure	-1.98
Right middle cerebellar peduncle	-1.95
Left superior cerebellar peduncle	-1.93
Right anterior commissure	-1.91

Note: Controls were identified with 77.4% accuracy, while COVID-19 subjects were identified with 85.2% accuracy (overall classification $p < .0001$).

the SVM model are depicted in a color-coded map (Figure 3B). Of note, the COVID-19 membership group did show blood flow abnormality predominantly in the frontal lobe, including the olfactory tubercle region.

In an attempt to identify a relationship between CBF and symptom severity in the COVID-19 sample, we conducted a separate SVR model using only participants in that group. Using this model, CBF data were also able to significantly predict COVID-19 severity after controlling for age ($R^2 = 0.1, p = .046$). Table 5 shows the top 20 areas predictive of severity in the SVR model.

DISCUSSION

Changes in CBF have been reported because of viral infections affecting the CNS. While originally thought to be a respiratory virus, neurological and long-term symptoms of COVID-19 implicate disruption to the central and peripheral nervous system. In the current study, we observed lower overall CBF in COVID-19-recovered individuals compared to age- and sex-matched control participants. Further

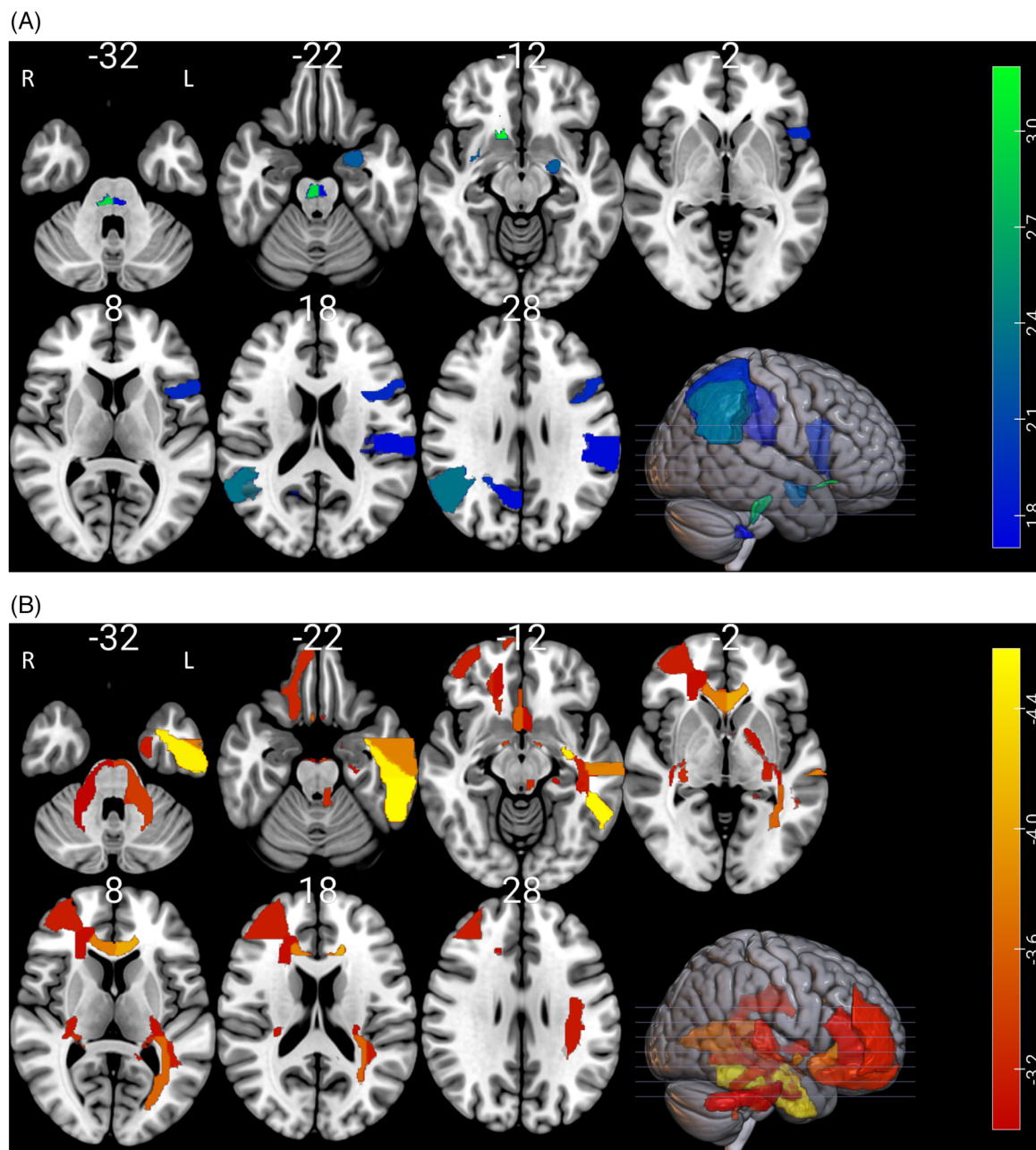


FIGURE 3 (A) Top 10 areas predictive of control group membership in the support vector machine (SVM) model (classification accuracy = 77.4%). (B) Top 10 areas predictive of COVID-19 group membership in the SVM model (classification accuracy = 85.2%). White numbers indicate axial slice location. The color bar represents z-scores for this contrast. Only statistically significant regions are shown. R, right; L, left.

analysis revealed robust differences in cerebral perfusion between the two groups in specific brain areas (frontal, temporal, and cingulate gyri as well as the basal ganglia) and WM tracts (including the lenticular fasciculus, cerebellar peduncles and others) (see Table 3). While severe cases of COVID-19 have resulted in millions of deaths, it is also important to understand the effects of surviving mild-to-moderate COVID-19 infection, which makes up approximately 80% of total cases.¹⁸ Even mild cases of COVID-19 can have long-term consequences that have a large cumulative effect on a population by altering diet, work, and ability to socially function. To date, most neurobiologi-

cal studies of COVID-19 have focused on brain changes associated with severe cases (ie, hospitalized or autopsy), and they have revealed ample evidence for neurological effects that may be related to brain inflammation and microbleeds,¹⁹ WM hyperintensities,²⁰ or neurotropism²¹ or have described the effects of COVID-19 on psychological factors, such as social isolation or posttraumatic stress.^{21,22} The current findings suggest that brain changes are not restricted to severe cases, with survivors of mild-to-moderate COVID-19 displaying altered CBF when compared to matched controls. Future studies should seek to determine if these alterations are associated with long-term

TABLE 5 List of regions most predictive of COVID-19 severity in the support vector machine model.

Top 10 regions where greater CBF was associated with greater COVID-19 severity	
Region	Feature weight
Right ansa lenticularis	1.91
Right hypothalamus	1.83
Left mammillary body	1.75
Left ansa lenticularis	1.67
Right genu of corpus callosum	1.67
Left corticospinal tract	1.59
Right body of corpus callosum	1.57
Left globus pallidus	1.48
Left pons	1.41
Right cingulum	1.41
Top 10 regions where less CBF was associated with greater COVID-19 severity	
Region	Feature weight
Left superior parietal gyrus	-2.06
Left middle frontal gyrus	-2.04
Right Meynert nucleus	-1.99
Left posterior middle temporal gyrus	-1.94
Left superior temporal gyrus	-1.83
Right nucleus accumbens	-1.81
Right pole of superior frontal gyrus	-1.76
Left Meynert nucleus	-1.76
Left superior frontal gyrus (prefrontal cortex)	-1.69
Right middle occipital gyrus	-1.51

Note: Values controlled for age ($R^2 = 0.1, p = .046$).

cognitive, behavioral, or health-related outcomes. These findings make sense in light of the known sequelae of COVID-19 and are discussed below. Observed abnormalities in perfusion of the basal ganglia and cerebral peduncles, which are both implicated in balance^{23,24} and dizziness,²⁵⁻²⁷ may be related to neurologic manifestations of dizziness in COVID-19.^{28,29} Similarly, changes in perfusion of the inferior frontal and olfactory tubercle, which are known to be related to odor detection and interpretation,^{30,31} may be related to alterations in the sense of smell reported in COVID-19.²⁸ Finally, changes in CBF identified in the frontal and temporal lobes and anterior cingulate, which are critical to high-level cognitive skills such as executive function³² and language processing,³³ may be related to reports of brain fog³⁴ and reports of potentially impaired speech processing³⁵ in COVID-19.

One interesting finding in this study is the high degree of accuracy with which our SVM-based predictive models were able to discriminate between participants with COVID-19 (~85% accuracy) and those never infected with COVID-19 (77% accuracy). To our knowledge, this is the first study that has attempted to predict COVID-19 infection status using an entirely brain-based approach. While other studies con-

ducted in clinical populations have validated the approach we used here (and additionally used it to predict continuous variables), similar predictive models for other similarly sized data sets do not typically achieve the same high level of accuracy we observed in the current study.^{15,16,17,36-39} As such, the current experiment is unique in that it identifies a robust, new biomarker for COVID-19 that follows known neurological and cognitive sequelae of infection. It would be interesting to apply this model to additional—perhaps larger—MRI data sets acquired in COVID-19, as well as to examine longitudinal changes in CBF associated with successful and impaired recovery.

While the results of this study are clear, the physiological mechanisms underlying the reported differences in CBF have yet to be established. To date, there is not a strong consensus regarding the relationship between vascular function and COVID-19 infection. One study reported blunted peripheral, but not cerebral, vasodilator function in long-haul COVID-19 patients. Information reported from other behavioral and brain imaging studies supports a link between COVID-19 and changes in blood flow, particularly in the brain. Campen and colleagues, for example, used the clinical tilt-test and extracranial Doppler to identify alterations in cerebral CBF in a sample of participants with COVID-19, concluding that CBF may be altered in this population.⁴⁰ Another recent paper describes alterations in both regional and whole-brain CBF as a result of mild to severe COVID-19 infections in hospitalized individuals.⁴¹ This research reported a moderate correlation between magnitude of brain changes, COVID-19 severity, and inflammatory markers including C-reactive protein, procalcitonin, and interleukin-6. While we did not measure inflammatory markers in the present study, we do report changes in CBF in a much milder group of COVID-19 infection than previous studies. We were also able to find a correlation between regional CBF and severity of COVID-19 in a nonhospitalized population. Interestingly, this model indicated that COVID-19 severity could be predicted by higher CBF in some areas, and lower CBF in other areas, stressing the fact that patterns of dysfunction—rather than global dysfunction—may be useful biomarkers of COVID-19 severity. While these results are not particularly robust (see limitations section below), and are not further discussed here, they do suggest the potential of using MRI-based metrics as an objective measures of brain function that may ultimately prove useful in prognosis of long-term neurological complications known to exist following COVID-19 even in mild cases (which include symptoms such as chronic fatigue, impaired cognition, dizziness, and alterations to the sense of smell/taste).

This study has some limitations that should be considered when interpreting the findings. We did not have information on duration and severity of COVID-19 infection. While we did find a significant correlation between region-specific CBF and COVID-19 severity in the current study, this effect was not particularly strong ($R^2 = 0.1$), corroborated by the low feature weights (Table 5) in the SVR analysis that predicts COVID-19 severity based on CBF data, and should be interpreted cautiously. In theory, we could improve this result by increasing our sample size, including hospitalized patients (extreme severity), or using a more sensitive, continuous (ie, noncategorical) measure of COVID-19 severity. Measuring severity via the immune



response or perhaps indirectly via quantification of inflammatory markers (which were not assessed in the current study) may also prove fruitful. Another important consideration is that participants with COVID-19 were scanned after the pandemic had officially been ongoing for months. Undoubtedly, the COVID-19 pandemic, and associated changes in diet, exercise, social interaction, mental health, and so forth, all of which are known to have effects on the brain, could be responsible for differences reported in the current study. With these considerations, it is possible to argue that our results speak to changes associated with the pandemic and COVID-19 infection. This would still be interesting and disentangling the effects of these two causes is certainly a topic for future, large-scale, preferably longitudinal, studies. Our participants, who were measured at the beginning of the pandemic, would have had the Delta strain of COVID-19, and other strains may have different effects on the brain. Finally, the fact that our sample consisted mainly of women (89%) limits our ability to generalize our results to men.

Despite these limitations, we report lower WM CBF, as well as widespread regional CBF changes identified using quantitative MRI, in mild COVID-19 patients. Further studies are needed to validate this newly identified COVID-19 imaging marker and determine whether CBF changes are related to changes in WM tracts and connectivity in COVID-19 patients.

ACKNOWLEDGMENTS

The authors have nothing to report.

CONFLICT OF INTEREST STATEMENT

The authors declare no conflicts of interest.

ORCID

Souvik Sen  <https://orcid.org/0000-0002-0886-2364>

Sarah Newman-Norlund  <https://orcid.org/0000-0002-9064-1332>

REFERENCES

- Lu R, Zhao X, Li J, et al. Genomic characterisation and epidemiology of 2019 novel coronavirus: implications for virus origins and receptor binding. *Lancet*. 2020;395:565–74.
- Kanberg N, Ashton NJ, Andersson LM, et al. Neurochemical evidence of astrocytic and neuronal injury commonly found in COVID-19. *Neurology*. 2020;95:e1754–59.
- Maltezou HC, Panagopoulos P, Sourri F, et al. COVID-19 vaccination significantly reduces morbidity and absenteeism among healthcare personnel: a prospective multicenter study. *Vaccine*. 2021;39:7021–7.
- Wolter N, Jassat W, Walaza S, et al. Early assessment of the clinical severity of the SARS-CoV-2 omicron variant in South Africa: a data linkage study. *Lancet*. 2022;399:437–46.
- Noguchi T, Yakushiji Y, Nishihara M, et al. Arterial spin-labeling in central nervous system infection. *Magn Reson Med Sci*. 2016;15:386–94.
- Ota K, Kimura M, Kawamoto M. Cerebral blood flow imaging in MR-negative SARS-CoV-2-related encephalitis with abnormal psychosis. *Eur J Nucl Med Mol Imaging*. 2022;49:2450–1.
- Ardellier FD, Baloglu S, Sokolska M, et al. Cerebral perfusion using ASL in patients with COVID-19 and neurological manifestations: a retrospective multicenter observational study. *J Neuroradiol*. 2023. <https://doi.org/10.1016/j.neurad.2023.01.005>
- Hacup ER, Hascup KN. Does SARS-CoV-2 infection cause chronic neurological complications? *Geroscience*. 2020;42:1083–7.
- Newman-Norlund RD, Newman-Norlund SE, Sayers S, et al. The Aging Brain Cohort (ABC) repository: the University of South Carolina's multimodal lifespan database for studying the relationship between the brain, cognition, genetics and behavior in healthy aging. *Neuroimage Rep*. 2021;1:100008.
- Rorden C, McKinnon E, Hanayik T, et al. Niipreprocess adapted for LARC and ABC studies at UofSC. Available from: https://github.com/neuroimabusc/nii_preprocess. Accessed 14 Dec 2022.
- Chappell MA, Groves AR, Whitcher B. Variational bayesian inference for a nonlinear forward model. *IEEE Trans Signal Process*. 2008;57:223–36.
- Smith SM, Jenkinson M, Woolrich MW, et al. Advances in functional and structural MR image analysis and implementation as FSL. *Neuroimage*. 2004;23:S208–19.
- Alsop DC, Detre JA, Golay X, et al. Recommended implementation of arterial spin-labeled perfusion MRI for clinical applications: a consensus of the ISMRM Perfusion Study Group and the European Consortium for ASL in Dementia. *Magn Reson Med*. 2015;73:102–16.
- Fonov VS, Evans AC, McKinstry RC, et al. Unbiased nonlinear average age-appropriate brain templates from birth to adulthood. *Neuroimage*. 2009;47:S102.
- Rorden C, McKinnon E, Hanayik T, et al. Niistat is a set of Matlab scripts for analyzing neuroimaging data from clinical populations. Available from: <https://www.nitrc.org/projects/niistat/>. Accessed 14 Dec 2022.
- Wernick MN, Yang Y, Brankov JG, et al. Machine learning in medical imaging. *IEEE Signal Process Mag*. 2010;27:25–38.
- Kristinsson S, Zhang W, Rorden C, et al. Machine learning-based multimodal prediction of language outcomes in chronic aphasia. *Hum Brain Mapp*. 2021;42:1682–98.
- Wu Z, McGoogan JM. Characteristics of and important lessons from the Coronavirus Disease 2019 (COVID-19) outbreak in China: summary of a report of 72 314 cases from the Chinese Center for Disease Control and Prevention. *JAMA*. 2020;323:1239–42.
- Kirschenbaum D, Imbach LL, Rushing EJ, et al. Intracerebral endotheliitis and microbleeds are neuropathological features of COVID-19. *Neuropathol Appl Neurobiol*. 2021;47:454–9.
- Egbert AR, Cankurtaran S, Karpiak S. Brain abnormalities in COVID-19 acute/subacute phase: a rapid systematic review. *Brain Behav Immun*. 2020;89:543–54.
- Song W-J, Hui CKM, Hull JH, et al. Confronting COVID-19-associated cough and the post-COVID syndrome: role of viral neurotropism, neuroinflammation, and neuroimmune responses. *Lancet Respir Med*. 2021;9:533–44.
- Fu Z, Tu Y, Calhoun VD, et al. Dynamic functional network connectivity associated with post-traumatic stress symptoms in COVID-19 survivors. *Neurobiol Stress*. 2021;15:100377.
- Surgent OJ, Dadalco OI, Pickett KA, et al. Balance and the brain: a review of structural brain correlates of postural balance and balance training in humans. *Gait Posture*. 2019;71:245–52.
- Boisgontier MP, Cheval B, Chalavi S, et al. Individual differences in brainstem and basal ganglia structure predict postural control and balance loss in young and older adults. *Neurobiol Aging*. 2017;50:47–59.
- Connor SE, Sriskandan N. Imaging of dizziness. *Clin Radiol*. 2014;69:111–22.
- Kim SH, Kim HJ, Kim JS. Isolated vestibular syndromes due to brainstem and cerebellar lesions. *J Neurol*. 2017;264:63–9.
- Schmahmann JD, Pandya DN. Disconnection syndromes of basal ganglia, thalamus, and cerebellar systems. *Cortex*. 2008;44:1037–66.
- Kishimoto-Urata M, Urata S, Kagoya R, et al. Prolonged and extended impacts of SARS-CoV-2 on the olfactory neurocircuit. *Sci Rep*. 2022;12:5728.



29. Romero-Sánchez CM, Díaz-Maroto I, Fernández-Díaz E, et al. Neurologic manifestations in hospitalized patients with COVID-19: the ALBACOVID registry. *Neurology*. 2020;95:e1060–70.
30. Yamaguchi M. Functional sub-circuits of the Olfactory system viewed from the olfactory bulb and the olfactory tubercle. *Front Neuroanat*. 2017;11:33.
31. Wesson DW, Wilson DA. Sniffing out the contributions of the olfactory tubercle to the sense of smell: hedonics, sensory integration, and more? *Neurosci Biobehav Rev*. 2011;35:655–68.
32. McDonald AP, D'Arcy RCN, Song X. Functional MRI on executive functioning in aging and dementia: a scoping review of cognitive tasks. *Aging Med*. 2018;1:209–19.
33. Friederici AD, Chomsky N, Berwick RC, et al. Language, mind and brain. *Nat Hum Behav*. 2017;1:713–22.
34. Hugon J, Msika EF, Queneau M, et al. Long COVID: cognitive complaints (brain fog) and dysfunction of the cingulate cortex. *J Neurol*. 2022;269:44–6.
35. Daroische R, Hemminghyth MS, Eilertsen TH, et al. Cognitive impairment after COVID-19—a review on objective test data. *Front Neurol*. 2021;12:699582
36. Yourganov G, Smith KG, Fridriksson J, et al. Predicting aphasia type from brain damage measured with structural MRI. *Cortex*. 2015;73:203–15.
37. Keator LM, Yourganov G, Basilakos A, et al. Independent contributions of structural and functional connectivity: evidence from a stroke model. *Netw Neurosci*. 2021;5:911–28.
38. Basilakos A, Rorden C, Bonilha L, et al. Patterns of poststroke brain damage that predict speech production errors in apraxia of speech and aphasia dissociate. *Stroke*. 2015;46:1561–6.
39. Wilmskoetter J, Fridriksson J, Basilakos A, et al. Indirect white matter pathways are associated with treated naming improvement in aphasia. *Neurorehabil Neural Repair*. 2021;35:346–55.
40. Campen CLMCV, Rowe PC, Visser FC. Orthostatic symptoms and reductions in cerebral blood flow in long-haul COVID-19 patients: similarities with myalgic encephalomyelitis/chronic fatigue syndrome. *Medicina*. 2021;58:28.
41. Qin Y, Wu J, Chen T, et al. Long-term microstructure and cerebral blood flow changes in patients recovered from COVID-19 without neurological manifestations. *J Clin Invest*. 2021;131:e147329.

How to cite this article: Sen S, Newman-Norlund R, Riccardi N, et al. Cerebral blood flow in patients recovered from mild COVID-19. *J Neuroimaging*. 2023;1–9.
<https://doi.org/10.1111/jon.13129>